Self consistent Shaw Optimized Model Potential Application to the determination of structural and atomic transport properties of liquid alkaline metals by molecular dynamics simulations.

Nadra Harchaoui, Slimane Hellal, Jean-Georges Gasser, Benoit Grosdidier

Self consistent Shaw Optimized Model Potential Application to the determination of structural and atomic transport properties of liquid alkaline metals by molecular dynamics simulations.

Journal:	*Philosophical Magazine & Philosophical Magazine Letters*
Manuscript ID:	TPHM-09-Sep-0402.R1
Journal Selection:	Philosophical Magazine
Date Submitted by the Author:	29-Oct-2009
Complete List of Authors:	Harchaoui, Nadra; Université de Tizi-Ouzou, Laboratoire de Physique et Chimie Quantique Hellal, Slimane; Université de Tizi-Ouzou, Laboratoire de Physique et Chimie Quantique Gasser, Jean-Georges; Université Paul Verlaine - Metz, LPMD; (personnal) Grosdidier, Benoit; Université Paul Verlaine - Metz, , Institut de Chimie, Physique et Matériaux
Keywords:	atomic structure, liquid metals, atomic transport, molecular dynamic simulations, diffusion
Keywords (user supplied):	model pseudopotentials

Self consistent Shaw Optimized Model Potential
Application to the determination of structural and atomic transport properties of liquid alkaline metals by molecular dynamics simulations.

N. Harchaoui [1, 2], S. Hellal [1, 2], J. G. Gasser [2, a], B. Grosdidier [2]

[1] Laboratoire de Physique et Chimie Quantique, Département de Physique, Faculté des Sciences, Université de Tizi-Ouzou, Campus de Hasnaoua, (15000) Tizi-Ouzou, Algeria.

[2] Laboratoire de Physique des Milieux Denses, Institut de Chimie, Physique et Matériaux, Université Paul Verlaine de Metz, 1 Bd D.F. Arago, 57078 Metz Cedex 3, France.

In this paper, we develop the "first-principle" Shaw full-nonlocal and energy-dependent Optimized Model Potential (OMP) [Phys. Rev. **174**, 1968]. Contrarily to the original paper, we obtain the OMP parameters in selfconsistent manner that doesn't ask for the knowledge of experimental values of the ionization and cohesive energies. To our knowledge it is the first time that this method is used for effective potential calculations. As an application to Li, Na, and K alkaline metals, we used OMP pseudopotential-based interactions between ions to carry out standard molecular-dynamics simulation. In these calculations, we first check the ionic structure for the liquid state at temperature near the melting point. Same accurate calculations, but for the atomic transport properties, predict the temperature dependence of the self-diffusion coefficients. Our theoretical results are in overall agreement with the available experimental measurements. Thus, one can have some confidence in the ability of the Optimized Model Potential to give a good representation of the physical properties of these alkaline ions in liquid environment.

Keywords: first-principle model potential, molecular dynamics, liquid metal, structure factor, self-diffusion.

I. Introduction

First-principle pseudopotentials remain up to today an important tool of investigation and have attracted several theoretical works [1-3]. Indeed, to understand the physical properties of simple metals from a fundamental point of view, one needs a quantum mechanic treatment of the metallic bond. This can be achieved by combining the pseudopotential formalism and electronic structure calculations with second-order perturbation recipes. This way leads to the "pair theory" for metals [4]

[a] Corresponding author. Email: gasser@univ-metz.fr

in which the interactions between ions are described in terms of an effective pairwise potential $V_{eff}(r)$. An interesting but stringent test of ability for the "pair theory" to accurately predict most of liquid state properties lies in the ionic structure calculation [4-7]. This one is given by the pair-correlation function $g(r)$ in real space or by the static structure factor $S(q)$ in the reciprocal one. It is closely conditioned by the shape of the ionic pair potential $V_{eff}(r)$. Furthermore, within the "pair theory" of fluids, it was shown that there is a one-to-one relationship between g(r) and $V_{eff}(r)$ [4,8]. However, a reliable test needs computer simulation method to bypass approximate theories of liquid state [4,5]. In the present work, we have firstly determined $g(r)$ and $S(q)$ for some alkali metals (lithium at 463 K, sodium at 378 K, and potassium at 338K). These two important functions are computed by using the molecular dynamic (MD) simulation technique [9] with the effective ionic pair potentials as main ingredients. We can already notice that $V_{eff}(r)$ and $S(q)$ play a central role in the physic of simple liquids. For instance, the microscopic theories of collective dynamics involve the use of precise form of $S(q)$ and of $V_{eff}(r)$ [10,11]. At the second stage, we have extended the pseudopotentiel-based calculations in order to investigate the atomic transport properties which are quite sensitive to the interactions. This task can be achieved through the calculated Velocity-Autocorrelation Function (VAF), the corresponding spectral density and the self-diffusion constant. Their temperature-dependence behavior in liquid state is discussed.

The ionic potentials are built within the framework of the first-principle pseudopotential formalism. We use the Optimized Model Potential (OMP) of Shaw [1] to describe the electron-ion interaction. Many-body effects in valence electrons gas are properly included through a full-nonlocal screening [12] of the bare electron-ion model with a suitable dielectric screening function [13,14] which has a good theoretical background. That is not without some difficulties due mainly to the nonlocal and energy-depending nature of the OMP-model [15-17]. We point out these difficulties in the pseudopotential context in section 2 where we will bring out the calculation of the OMP parameters as a central problem. For clarity needs, we briefly remind in section 3 some quantitative aspects of the ionic structure and of the self-diffusion for pure liquid metals. In the same section, we will also present the computing conditions with the standard molecular dynamics. In the last section 4, the essential features of the calculated pair potentials $V_{eff}(r)$ and the behavior of the structural quantities $g(r)$ and $S(q)$ for the studied alkaline metals will be discussed in connection with the energy-dependence of OMP parameters. Next to this, we will report and interpret our theoretical results upon other quantities that provide detailed and systematic microscopic understanding of the self-diffusion phenomena in liquid state.

(Unless explicitly stated otherwise, later on we use atomic units throughout: $\hbar = m = e = 1$)

II. The Optimized Model Potential of Shaw: theoretical background

A. Model Potential for free ion

Axiomatic principles of the pseudopotential method within the plane-wave-basis formalism are well-known and are described in a number of monographs and textbooks [2,3,18,19]. The main goal of this method is to remove the core states in the electronic structure calculations so that the strong full-electron potential in the one-electron Schrödinger-type equation is replaced by an effective much weaker potential, namely the "pseudopotential". There are many ways to construct pseudopotentials (see brief review in [3,19]). During the last three decades they have been generated from all-electron calculations for a free atom so that their main scattering properties are captured [20-24]. Such scattering properties can be indeed rephrased in terms of logarithmic derivatives arguments [20,21]. However, these atomic calculations involve various underlying problems that can spoil the quality of the pseudopotential. Most of them are mainly associated with non-linear aspects of density-functional exchange-correlation-energy [25]. Much more, "transferability" of the bare ion pseudopotential [21] can be also altered as regard to some other considerations such as the Kleinmann and Bylander factorization [22,26] or the "chemical hardness" criterion [27]. In addition, Hafner [7] already stressed the fact that «the use of norm-conserving pseudopotentials [20,21] in perturbation calculations yields some serious problems». If one now turns to alkali metals, Na is a prototype element in the field of application of the pseudopotential theory. However, unlike Na which is an ideal case, light element Li, having strong pseudopotential, requires great attention in the atomic calculations [23]. Previously, Shenoy and Halder [28] have emphasized the singularity of Li ion. The latter, without p-core states, must be described by a nonlocal pseudopotential. To elude the difficulties which appear when we dealt with *ab initio* pseudopotential, we performed our electronic structure calculations using OMP-model potential of Shaw [1,15-17]. This model is built in the spirit of the "Quantum Defect Method" [29] so that it matches to the observed atomic energy levels of the isolated ion [30]. In this approach, difficulties about exchange and correlation with the core electrons are somewhat minimized [18]. The real-space representation of Shaw's bare-ion OMP-model potential reads:

$$\hat{w}_{ion}^{0} = -\frac{z_V}{r} - \sum_{\ell=0}^{\ell=\ell_0} w_\ell^{ion}(r)\,\hat{P}_\ell\,, \qquad (2.1)$$

where z_V stands for the nominal valence and ℓ_0 is the highest value of ℓ-angular momentum in the core (typically: $\ell_0 = 0, 1$ or 2). The expressions of the ℓ-angular momentum component $w_\ell^{ion}(r)$ of the bare ion model potential and of the angular momentum projection operator $\hat{P}_\ell$ are:

$$w_\ell^{ion}(r) = \Theta(R_\ell - r)\left[A_\ell(E) - \frac{z_V}{r}\right], \quad \text{with} \quad \hat{P}_\ell = \sum_{m=-\ell}^{m=\ell} |\ell,m\rangle\langle\ell,m| \qquad (2.2)$$

Here $\Theta(R_\ell - r)$ the function of Heaviside (this one is unity for $R_\ell > r$ and zero otherwise) and $|\ell, m\rangle$ stands for the normalized spherical harmonics. The energy-dependent well depths $A_\ell(E)$ have been accurately evaluated at the ionic spectroscopic terms. In accordance with Shaw optimization requirement, the pseudizing radii $R_\ell(E)$ are related to the first ones through the following "optimization" relationship: $R_\ell(E)\, A_\ell(E) = z_V$ (2.3)

B. Model Potential for a metal

We consider now a homogeneous metallic medium at observed density, so that, the valence charge z_V, the atomic volume Ω_0, the atomic radius R_a such as $\Omega_0 = 4\pi R_a^3/3$, the electronic number density "n", the Fermi momentum $k_F = (3\pi^2 n)^{1/3}$, and the electron-sphere radius $r_s = R_a z_V^{-1/3}$ are then well-defined. So, to describe valence-electron-ion interaction in a metal environment using OMP-model is not an easy task mainly because it depends on the energy on an absolute scale. As a preliminary step, the OMP-model parameters must be evaluated at the valence energy $E_{\vec{k}}$ in the metal shifted by an amount $\Delta E_{\vec{k}}$ namely at $E^*_{\vec{k}} = E_{\vec{k}} - \Delta E_{\vec{k}}$. Because it is found that model parameters have rough linear energy-dependence, Animalu and Heine [31] gave a faithful procedure for the pure metal case. Indeed, let us consider with a high degree of accuracy, that:

$$A_\ell(E^*_{\vec{k}}) = A_\ell(E^*_F) + (E_{\vec{k}} - E_F)\left(\frac{\partial A_\ell}{\partial E}\right)_{E^*_F} \tag{2.4}$$

In (2.4) we have considered that at first approximation, the "core shift" $\Delta E_{\vec{k}}$ doesn't depend on energy level. Hence one need the Fermi energy level E_F and the associated "core shift" ΔE_F to be estimated in order to calculate the shifted Fermi energy $E^*_F = E_F - \Delta E_F$. To do this, Animalu and Heine gave an explicit but crude approximations for E_F and ΔE_F:

$$E_F = -|MIE| - |BEE| + \frac{2}{5}\left(\frac{k^2}{2m}\right) + \frac{0.6 Z_v^{2/3}}{r_s} - \varepsilon_{xc} + \mu_{xc} \tag{2.5}$$

$$\Delta E_F = \mu_{xc} + \frac{Z_v}{2r_s}\left[3 - \frac{3}{4}\left(\frac{R_M}{r_a}\right)^2\right] \tag{2.6}$$

where ε_{xc} is the exchange-correlation energy per electron for a homogeneous electron gas. Within LDA approximation, the exchange-correlation potential can be obtained as: $\mu_{xc} = \varepsilon_{xc} - \frac{r_s d\varepsilon_{xc}}{3dr_s}$. For the unpolarized gas, we have: $\varepsilon_{xc} = \varepsilon_x + \varepsilon_c$. If the exchange energy per electron is well known to be

$\varepsilon_x = -0.45817/r_s$, several interpolation formulas for the correlation energy ε_c are available in the literature. Since our present calculations otherwise performed will be compared with previous work of Cowley [32], it may a good thing to recall that this author used the one given by Nozières and Pines [33]: $\varepsilon_c = -0.0575 + 0.0155\,\mathrm{Ln}\left(r_s\right)$. Cowley made essentially the comparison between his results as obtained from (2.6) to those calculated when he made allowance for the first Ballentine and Gupta [34] correction to last term of (2.6). Cowley has also considered subsequent additional correction suggested by these same authors. By necessity, OMP calculations issued from the original procedure devised by Animalu and Heine are later on denoted OMP-AH while those referring to Ballentine and Gupta schemes are recognized, respectively as OMP-BG1 and OMP-BG2. In any case, the shift ΔE_F involves the values of core radius R_M. At our knowledge, there are no theoretically well-founded arguments that yield to any convenient expression for R_M. In the past, Ese and Reissland chose it to be model-dependent and posed $R_M = Z_v / A_\ell\left(E_F^*\right)$. Hence to estimate $A_0\left(E_F^*\right)$, equations (2.5) and (2.6) together are solved iteratively. We think that this scheme is inconsistent since it doesn't lead to a unique determination of E_F^*. On the other hand, Cowley assuming that $R_M = Z_v / A_0\left(E_F^*\right)$ performed similar iterative scheme to get $A_\ell\left(E_F^*\right)$ with clearly a unique value of E_F^*. Nevertheless, one can note that in all respects Cowley assumption is arbitrary. Upon the whole, the previous procedures requiring the knowledge of the mean ionization energy (MIE) and of the binding energy per electron (BEE) yet has drawback. Unfortunately, there are no available data of BEE for any thermodynamic state. We believe that the values tabulated by Ese and Reissland [35] and those calculated by Cowley concern solely the solid state. Thus the evaluation of the Fermi energy on the absolute scale and of the core shift remains an intricate problem. To overcome this difficulty and following upon previous pioneer work of Taut and Paasch [36], Hallers *et al.* [37] have devised a procedure in which OMP-model parameters $A_\ell\left(E_F^*\right)$ at the shifted Fermi energy, are directly evaluated in the selfconsistent manner within the first order pseudopotential-perturbation theory. This method has only be used for electronic transport properties [37] through the electron ion interaction, never for atomic structure and atomic transport through the ion ion effective potential. It turns out that from this selfconsistent calculation of $A_\ell\left(E_F^*\right)$, for which we use the abbreviation OMP-Self, the binding energy per electron BEE can be conversely estimated accounting of either the Animalu and Heine procedure or the Ballentine and Gupta ones. Before, equation (2.4) must be solved for:

$$E_F^* = \frac{A_\ell\left(E_F^*\right) - A_\ell(0)}{\left(\frac{\partial A_\ell}{\partial E}\right)_0} \qquad (2.7)$$

Our OMP-Self parameters $A_\ell\left(E_F^*\right)$ for Li, Na and K are gathered in Table I along with previous theoretical results of Cowley. This author used the three like Animalu and Heine procedures denoted above OMP-AH, OMP-BG1, and OMP-BG2. We note that OMP-Self, OMP-AH, and in some measure OMP-BG1, respective calculations fairly converge. On the other hand, we agree with Cowley that « the inclusion of the particular form of inhomogeneity correction » given by Ballentine and Gupta (OMP-BG2) leads to « a gross shift in the absolute energy of the conduction band ». Further, we will confirm this statement. In the last column of table I, we also report the crude estimate of BEE issued from our accurate OMP-Self calculation of $A_\ell\left(E_F^*\right)$ together with the use of equations (2.5), (2.6) and (2.7). We wish to point out that our predicted BEE for Li is in a close agreement with experimental data. On the other hand, the result for Na is rather less good and the K one's turns only qualitative.

Since OMP-model is a nonlocal operator that also depends on the energy, the implementation of electronic structure calculation is not straightforward. First, we have dealt with some other cumbersome concepts that are closely linked to the energy dependence of the OMP-model. It is not convenient here to dwell too long upon these. Their signification and their importance are widely stressed in the literature. Shaw [16] introduced effective valence z_v^*, and effective masses $m_{\vec{k}}$ and $m_E\left(\vec{k}\right)$. However, the depletion hole [15] n_d that is also a manifestation of the energy-dependence of the OMP-model, accounts for the difference between the true and pseudo-charge densities in the metals. It is instructive to note that the expression for the depletion hole given by Shaw and Harrison [15], equation (2.8) in this reference, is closely related to the Friedel "sum rule" and so to the scattering properties. Another crucial problem is connected with the many-body effects among electron-valence gas. These ones are incorporated in sitting up the OMP-screened-model potential. To do accurate calculations taking account of the nonlocal nature and energy-dependence of the OMP-model, one used full-consistent screening [12,17] with the "electron-test-charge dielectric function" $\varepsilon(q)$ and the local-field correction function $G(q)$ [13,14]. To include the exchange and correlation, the electric dielectric function $\varepsilon(q)$ is related to the Hartree dielectric function $\varepsilon_H(q)$ following the relationship:

$$\varepsilon = 1 + \frac{1}{(m_E(k_F))^2}(1-G)(1-\varepsilon_H) \qquad (2.8)$$

where $\varepsilon_H = 1 + \frac{2}{\pi k_F \eta^2}\left\{1 + \frac{4-\eta^2}{4\eta}\mathrm{Log}\left(\frac{2+\eta}{2-\eta}\right)\right\}$, and $\eta = \frac{q}{k_F}$. In (2. 8), $m_E(k_F)$ specifies the Shaw effective mass evaluated at the Fermi momentum. Among the most well-physically-based forms for $G(q)$ at the present time (see, e. g., ref [14]) we have chosen to use in our calculations the one of Ichimaru and Utsumi [13].

We now again consider the bare model potential for an ion implanted in a liquid metal. As it is previously emphasized, in the metal environment its parameters must be evaluated at the valence energy $E_{\vec{k}}$ shifted by $\Delta_{\vec{k}}$ namely at $E_{\vec{k}} - \Delta_{\vec{k}}$. In the second-order perturbation theory, one has need of the matrix element of the bare model potential that is to say:

$$N\left\langle \vec{k}+\vec{q}\left|\hat{w}_{ion}^{0}\right|\vec{k}\right\rangle = v_q + f_{\vec{q}\vec{k}} \tag{2.9}$$

The so-called unscreened-form factor (2.9) contains two matrix elements v_q and $f_{\vec{q}\vec{k}}$ which correspond to respectively the local and to the nonlocal parts of the bare model potential. If the complex expression for $f_{\vec{q}\vec{k}}$ can be found in the Shaw paper [1], v_q can be deduced from the simple form:

$$v_q = -\frac{4\pi z_V}{\Omega_0 q^2} \tag{2.10}$$

The corresponding matrix element of the screened model potential or screened form factor is also useful. It takes the following expression [39]:

$$N\left\langle \vec{k}+\vec{q}\left|\hat{w}_{ion}\right|\vec{k}\right\rangle = \frac{w_{0q}}{\varepsilon(q)} + f_{\vec{q}\vec{k}} + g(q) \tag{2.11}$$

In (2.11) the term w_{0q} is a sum of the local potential due to the valence charge v_q (2.10) and that due to the renormalized depletion hole v_{dq}. This last is corrected by exchange and correlation through [39] $G(q)$ so that,

$$w_{0q} = v_q + (1-G)v_{dq} \tag{2.12}$$

where:

$$v_{dq} = \frac{4\pi n_{dq}}{m_E \Omega_0 q^2} \tag{2.13}$$

If we know the spatial distribution of the depletion hole $n_d(r)$ and its Fourier transform n_{dq}, expression (2.13) for v_{dq} arises from the Poisson theorem. Unfortunately, model-potential theory does not provide $n_d(r)$. We used at best this degree of freedom assuming that the depletion hole is uniformly distributed within a spherical shell whose radius R_C is a weighted mean of $R_\ell(E)$ model radii [40]. With this choice, the normalized pseudo-wave-function and the normalized eigenfunction have same shape and same amplitude in the region outside the sphere, like that must be. If we define here the modified Coulomb factor as $v_c^* = \frac{4\pi}{q^2}[1-G]$, the nonlocal screening contribution $g(q)$ in (2.11) may be then written:

$$g(q) = \frac{v_c^*}{2\pi^3 \varepsilon} \int_{\Omega_F} \frac{f(\vec{q},\vec{k})}{m_{E(\vec{k})} m_{E(\vec{k}+\vec{q})} (E_{\vec{k}}^0 - E_{\vec{k}+\vec{q}}^0)} d^3\vec{k} \tag{2.14}$$

The $g(q)$ function accounts for the exchange-correlation effect and energy-dependence of the OMP-model potential. This definition of $g(q)$ [39] is otherwise different in comparison with Shaw's one [16]. The first order in expansion for the energy of electronic states in perturbation theory is given in terms of effective masses as follows [16]:

$$E^{o}_{\vec{k}} = \frac{k^2}{2m_{\vec{k}} m_{E(\vec{k})}} \tag{2.15}$$

C. Effective interatomic pair potential

From the first-principle model potential presented above, one can determine the effective pair potential $V_{eff}(r)$ between an ion and another one in liquid metal. The second-order perturbation theory together the pseudopotential formalism leads to the familiar expression [7,39,41]:

$$V_{eff}(r) = \frac{\left[z^{*}_{v}\right]^2}{r}\left[1 - \frac{2}{\pi}\int_0^{\infty} F_N(q)\frac{\sin(qr)}{q}\right]dq \tag{2.16}$$

This pair potential is connected to the model pseudopotential via the so-called normalized energy-wave-number characteristic $F_N(q)$ [7,39,41]. The bare model potential for ions is suitably screened, taking account properly of its nonlocal and energy-dependent nature (full-nonlocal screening). The core shift is self-consistently evaluated according to the procedure that Hallers *et al.* [37] used for electronic transport calculation. To our knowledge it is the first time that this method is used for effective potentials. Hence, $F_N(q)$ has the very complex expression [6,13,39]:

$$F_N(q) = -\left(\frac{\Omega_0 q^2}{4\pi\pi^{*}_{v}}\right)^2 \frac{1}{1-G}\left\{\frac{1-\varepsilon}{\varepsilon} w^2_{0q} + 2w_{0q}g + \varepsilon g^2 + h - G(1-G)\, v^2_{dq}\right\} \tag{2.17}$$

Except the term $h(q)$, all quantities in this equation are defined in the precedent subsection. As for $g(q)$ defined by (2.14), the $h(q)$ function arises from the nonlocal part of the bare-ion OMP-model. By including exchange-correlation effect and effective masses, it can be written [39]:

$$h(q) = \frac{v^{*}_{c}}{2\pi^3}\int_{k\le k_F} \frac{f^2(\vec{q},\vec{k})}{m_{E(\vec{k})} m_{E(\vec{k}+\vec{q})}(E^0_{\vec{k}} - E^0_{\vec{k}+\vec{q}})} d^3\vec{k} \tag{2.18}$$

So, within the "pair theory" of liquid metals, the effective pair potential (2.16) can be employed later on to describe the atomic structure and the self-diffusion phenomena.

III. Structural and atomic transport properties: molecular dynamics simulation

In order to check the accuracy of the pair potentials (2.16) that are built within pseudopotential formalism previously described, we used molecular dynamics simulations to solve the classical equations of motion for a system of N atoms interacting via these potentials. So, provided atomic positions $\vec{r}_\alpha(t)$ and velocities $\vec{v}_\alpha(t)$ at time t for each particle «α», we can examine the atomic structure and transport properties for liquid metal. First we check the pair-correlation functions $g(r)$ computed as the time average [9]:

$$g(r) = \frac{1}{\rho}\left\langle \sum_{\alpha=1}^{N} \Delta N_\alpha(r, r+\Delta r) \Big/ \left(4\pi r^2 \Delta r\right) \right\rangle \tag{3.1}$$

Above, ΔN_α stands for the number of the atoms in the distance between r and $r+\Delta r$ from the atom «α», and henceforth ρ will be the average number density at given temperature T. The corresponding static structure factor $S(q)$ is obtained through the Fourier transformation [6]:

$$S(q) = 1 + \rho \int [g(r) - 1] \exp(-i\vec{q}\,.\,\vec{r})\, d^3\vec{r} \tag{3.2}$$

In the methods of computer simulation, one considers a periodic system of cell side L. To be consistent with that, the r-range values for the calculated radial distribution functions $g(r)$ is only significant up to $L/2$. So, its truncation in the Fourier transformation leads to spurious oscillations in $S(q)$ at small q-values. Such effects can be problematic if we wish to extrapolate the long-wavelength limit $S(0)$. It is well-known that this limit relates the atomic structure to the isothermal compressibility [4,5]. So, instead of equation (3.2), the structure factor can be directly computed from canonical averages over the successive atomic configurations of the atomic positions $\{\vec{r}_\alpha\}$ that are generated by MD simulation and over all $\vec{q}$ vectors of the same magnitude. Explicitly we have:

$$S(q) = \left\langle \rho_{\vec{q}} \rho_{-\vec{q}} \right\rangle \quad \text{with} \quad \rho_{\vec{q}} = \frac{1}{\sqrt{N}} \sum_{\alpha=1}^{N} \exp[i\vec{q}.\vec{r}_\alpha] \tag{3. 3}$$

Unfortunately, from equation (3.3) we observe that only the reciprocal lattice vectors $(n_x, n_y, n_z)2\pi / L$ are accessible and meaningful [42]. So that, the smallest q-value is $4\pi/L$. This indicates that the density fluctuations cannot be examined over distances larger than L/2.

We now consider succinctly the atomic transport properties without using more fundamental theories. The same recorded-atomic configurations allow us to calculate the self-diffusion constant D at given

temperature from the behavior of the mean square displacement $\left\langle \Delta r^2(t) \right\rangle$ at large t through the well-known Einstein relation [4,5]:

$$D = \lim_{t\to\infty} \frac{1}{6t} \left\langle \Delta r^2(t) \right\rangle \quad (3.4)$$

with:

$$\left\langle \Delta r^2(t) \right\rangle = \frac{1}{N} \left\langle \sum_{\alpha=1}^{N} |\vec{r}_\alpha(t) - \vec{r}_\alpha(0)|^2 \right\rangle \quad (3.5)$$

The self-diffusion constant D can also be extracted from the recorded atomic velocities $\vec{v}_\alpha(t)$ at time t, by integral over the velocity autocorrelation function (VAF) $Z(t)$ defined as follows [4,5]:

$$Z(t) = \frac{1}{3N} \sum_{\alpha=1}^{N} \left\langle \vec{v}_\alpha(t) \cdot \vec{v}_\alpha(0) \right\rangle \quad (3.6)$$

So that we have the Green-Kubo like equation for the self-diffusion constant:

$$D = \int_0^\infty Z(t)\,dt \quad (3.7)$$

The equipartition theorem implicates that $Z(0) = \frac{k_B T}{M}$ where M, k_B and T are the particle mass, the Boltzmann constant, and the temperature, respectively. Hence it is often convenient to define the normalized-VAF:

$$Z_N(t) = Z(t)/Z(0) \quad (3.8)$$

The velocity autocorrelation function on an equal footing with it corresponding spectral function $Z(\omega)$ almost provides essential information upon the diffusion process in liquid metal. It is obtained from Fourier transformation with respect to time:

$$Z(\omega) = \int_{-\infty}^{+\infty} Z(t) \exp(-i\omega t)\,dt \quad (3.9)$$

The integral over ω is simply $\frac{2\pi k_B T}{M}$ and the self-diffusion coefficient can be obtained as the zero-frequency limit:

$$D = Z(0) \quad (3.10)$$

Present standard molecular dynamics calculations using Verlet algorithm [9] have been carried out for a (NVT)-ensemble with 4000 atoms enclosed in a cubic supercell with periodic boundary conditions. The cubic cell size L is chosen so that it corresponds to the observed number density ρ at the given temperature (L=44.8 Å corresponding to ρ= 0.04458 atoms/Å^3 at T=463K for lithium, L=54.5Å corresponding to ρ =0.02486 atoms/Å^3 at T=378 K for sodium, and L=68.1 Å corresponding to ρ=0.0 1276 atoms/Å^3 at temperature T=338 K for potassium). The ionic pair potentials that we have used have been truncated at the cut-off radius close to L/2. In order to avoid any memory effect, we have carried out an annealing simulation by checking several MD-runs at different high temperatures (up to 5000K). To obtain accurate MD calculations, the equations of motion are integrated with MD-

time steps less than 1 fs. The number of such steps ($N_{steps} = 36000$) is large enough to ensure accurate calculations of the static liquid structure and transport properties. We thus obtain reliable pair correlation function $g(r)$ and from equation (3.2) accurate static structure factor $S(q)$. We sometimes use equation (3.3) in order to check the accuracy upon $S(q)$ at long wavelengths. In this case, molecular dynamics calculations for a (NVT)-ensemble are performed with only 864 atoms. These calculations with 864 atoms are relatively accurate to study the diffusion properties.

IV. Results and discussion

A. The static ionic structure versus interatomic pair potentials

The accurate interatomic pair potentials for Li, Na and K liquid metals at temperature near the melting point (463 K, 378 K and 338 K respectively) are derived from the electronic structure calculations by using Shaw's nonlocal and energy-dependent OMP-model potential. The bare ion model is suitably screened by the dielectric function, taking account of its nonlocal nature and its energy-dependence, so that, among various forms of the local field-correction seen in the literature, we retain the one having a physically well-based background proposed by the Ichimaru and Utsumi. Hence, it appears clearly from our preliminary investigations that for alkali metals the ionic structure and the atomic transport properties depend moderately on the valence-exchange and correlation potential. We can draw the same conclusion with regard to the precise form of the depletion charge distribution. The latter has a weak impact on our results. As it, has been said earlier (see section II), we have considered it uniformly distributed within a spherical shell with radius R_C On the other hand, the manner to deal with the "core shift" in order to obtain the well depths $A_\ell(E)$ of the bare ion model potential is crucial (see section II). These one are calculated self-consistently (OMP-Self) or evaluated according to either the Animalu-Heine original approach (OMP-AH) or by one or the other of the two Ballentine-Gupta corrections to Animalu-Heine Scheme (OMP-BG1, OMP-BG2).

We note that the shape of the interatomic pair potential is quite sensitive to the magnitude of energy-dependent well depths $A_\ell(E)$. This statement for the liquid sodium case is depicted in fig. 1. From this figure, it is fair to say that both approaches denoted OMP-Self and OMP-AH, seem to be reasonably convergent. Comparatively, OMP-BG1-derived pair potential is slightly shifted toward the smallest inter-particle distances. However, this situation is not dramatic and all three approaches lead to calculated pair correlation curves $g(r)$ (fig. 2) and to ones of the corresponding static structure factor $S(q)$ (fig. 3) that are almost identical. One point deserves noticed is that these theoretical results successfully predict the experimental data [6,43,44]. On the other hand, OMP-BG2 calculations reported in fig. 1, yield pair potential that exhibits a marked shift of the first minimum to smaller inter-particles distances. Consequently, it has an unrealistic much smaller diameter of the repulsive core.

So, the large discrepancies between predicted ionic structure from OMP-BG2 and the experiment are not surprising (figs. 2 and 3). To be compared, the OMP-Self-derived interatomic-pair potentials for Li and for K are plotted in fig. 4 together with the Na-one. Apart from a scaling factor, they are not significantly different. As one would expect, they show overall features that are typical of alkali metals. They consist of a strongly repulsive core at short distances plus an oscillatory tail at intermediate and long distances. These so-called "Friedel oscillations" with much damped amplitude at large r, are due to the logarithmic singularity of the dielectric function (2.8). It is worth to note that all potentials exhibit a deep negative minimum around the nearest neighbor typical distance: (Li : $R_{min} = 3.16\text{Å}$, $V_{min} \cong -74$ meV; Na : $R_{min} = 3.68\text{Å}$, $V_{min} \cong -44$ meV; and for K : $R_{min} = 4.52\text{Å}$, $V_{min} \cong -40$ meV). The similarity of the potentials is reflected in the pair-correlation functions $g(r)$ (for the needs of clarity, those of Li and K are not reported in this paper), whereas the respective static structure factors $S(q)$ are represented in figs. 5 and 6. Both functions have the main features of the hard-sphere-like structure. All curves also show an overall good agreement between our theoretical results and experimental ones [6,43-45].

B. Some properties of diffusion

Our results relative to the normalized VAF's for the three alkaline metals (Li, Na and K) in the liquid state are displayed in figs. 7. We may note at once that for all elements the main feature of the curves is characteristic of dense fluids, i.e. a damped-oscillatory behavior with negative regions. Negative regions are meaningful of thermal vibrating motion of an ion surrounded by others ions ("caging" effect). The picture is the one of a tagged particle which come into collision with near neighbors so that its velocity is, on average, in the reverse direction (backscattering). The magnitude of the oscillations so quickly decreases that only the first and the second oscillations both are apparent. Besides, with the increase in temperature the damping is more important. It can even be so pronounced that the normalized VAF becomes almost monotonically decreasing without the first negative minimum. The example of potassium at 800 K illustrates this fact. In addition, one can notice that the magnitude of the first minimum is sensitive to the atomic mass. As regard the sequence (Li, Na, K), the depth is decreasing with the mass of diffusing atom. Now, let us consider the corresponding spectral density functions $Z(\omega)$ represented in figs. 8. As VAF, spectral density function describes atomic motion that is both diffusive and vibrational. A quick look reveals that, as one could expect, $Z(\omega)$ is non-negative and has a finite value at zero frequency. Clearly, at temperatures just above the melting point, all curves relative to Li, Na, and K metals display a hump around 40, 15 and 8 ps^{-1}, respectively. As the temperature increases this one flattens until to behave a bare shoulder. We wish to point out that our molecular dynamic results of VAF's and of corresponding spectral $Z(\omega)$ densities agree quite well with other calculations [46]. Only the self-

diffusion constants, as we derived from the integration of VAF's (Equation 3.7), are reported in fig. 9 and summarized in Table II. Indeed, except some systematic deviations due to the computational conditions and that are upon the whole negligible, the D-values thus- obtained are consistent with those extracted from the Einstein relation (Equation 3.4) or founded upon the zero-frequency limit of spectral function $Z(0)$ (Equation 3.10). The values of D calculated for Li, Na, and K at temperatures 463, 378, and 343 K, respectively are explicitly reported in table II and compared with experimental results [47]. In regard to the variation over a wide range of temperatures, it is convenient to fit the numerical results by considering Arrhenius' type behavior of the form $D(T) = D_0 \exp\left(-\frac{Q}{RT}\right)$; R being the perfect gas constant. To compare our results to other calculations and to available measurements, we plot in fig. 9 $\mathrm{Ln}(D)$ as a function in inverse temperature, so that the pre-exponential factor D_0 and the activation-like energy Q can be extracted (see table II). Broadly speaking, our results agree well with measurements [4,47] on the entire temperature-range that we have considered.

V. Summary

Through the theoretical results reported in this paper, we intended to understand and to describe both the ionic structures and the diffusion phenomena for three alkali liquid metals. The successful process requires microscopic models of interatomic interactions. The theoretical tools involved are fully justified. At the beginning, and to avoid dealing with the limited knowledge of valence-core exchange and correlation and with other complications arising from first-principle pseudopotentials, we used Shaw's bare ion optimized model potential. The task was rather less straightforward on account of the nonlocal nature and energy-depending of the selected model. With respect to the calculation of the model's parameters, the drawbacks of usual procedure are enlightened. First, we overcame these difficulties by treating the core-shift problem following the ingenious method of Hallers *et al.* It is fair to say that this self-consistent method (OMP-Self) and Animalu-Heine's (OMP-AH) seem to be reasonably convergent. Second, we accounted for collective aspects of the valence-electrons by using the realistic screening-function of Ichimaru and Utsumi. Ultimately, the model is fully-screened in the second-order-perturbation theory. The pairwise derived potentials lead to an astonishing accuracy of the MD-calculated-ionic structure for Li, Na and K liquid metals. Moreover, it proves that first-principle pseudopotential-derived pair theory with OMP model accounts reasonably for atomic transport properties. With regard to the present calculations that we are the first to perform at our knowledge, we can reasonably claim that in some sense the "transferability" of the Shaw model potential to a liquid alkaline-metal environment is settled. However, we are aware that our concluding

remark will better be strengthened by the investigation of the dynamic structure factor $S(q,\omega)$ and related properties. These results also prompt us to extend such calculations for alkali-based liquid alloys.

References

[1] R.W. Shaw Jr, Phys. Rev. 174 (1968) p.769.

[2] W.A. Harrison, *Pseudopotentials in the Theory of Metals*, Benjamin, New York, (1966).

[3] G.B. Bachelet, *Strategies for Computer Chemistry*, C. Tosi (ed.) by Kluwer Academic Publishers (1989) p.119 -160.

[4] P.A. Egelstaff, *An Introduction to the Liquid State*, Clarendon Press, Oxford, 2nd ed., (1994).

[5] J.P. Hansen and I.R. McDonald, *Theory of Simple Liquids*, London: Academic Press, (1976).

[6] Y. Waseda, *The Structure of Non-crystalline Material: Liquid and Amorphous Solids*, McGraw-Hill, New York, (1980).

[7] J. Hafner, *From Hamiltonians to Phase Diagrams*, Springer-Verlag, New York, (1987).

[8] C.G. Gray and K.E. Gubbins, *Theory of Molecular Fluids*, Clarendon Press, Oxford. (1984).

[9] M.P. Allen and D.J. Tildesley, *Computer Simulation of Liquids*, Oxford Sci. Pub. (1987).

[10] A. Monaco, T. Scopigno, P. Benassi, A. Giugni, G. Monaco, M. Nardone, G. Ruocco and M. Sampoli, J. Non-Crystalline Solids. 353 (2007) p. 3154.

[11] S. Singh, J. Sood and K. Tankeshwar, J. Non-Crystalline Solids. 353 (2007) p. 3134.

[12] A.O.E. Animalu, Phil. Mag. 11 (1965) p.379.

[13] S. Ichimaru and K. Utsumi, Phys. Rev. B 24 (1981) p.7385.

[14] S. Hellal, J.G. Gasser and A. Issolah, Phys. Rev. B 68 (2003) p.094204.

[15] R.W. Shaw Jr and W.A. Harrison, Phys. Rev. 163 (1967) p.604.

[16] R.W. Shaw Jr, J. Phys. C2 (1969) p.2350.

[17] R.W. Shaw Jr, J. Phys. C3 (1970) p.1140.

[18] V. Heine, in *Solid State Physics*, edited by H. Ehrenreich, F. Seitz, and D. Turnbull , Academic, New York, (1970), Vol. 24, p.1.

[19] M.L. Cohen and J. R. Chelikowsky, *Electronic Structure and Optical Properties of Semiconductors*, 2nd ed., Springer-Verlag, Berlin, (1988).

[20] D.R. Hamann, M. Schlüter and C. Chiang, Phys. Rev. Lett. 4 (1979) p.1494.

[21] G.B. Bachelet, D.R. Hamann and M. Schlüter, Phys. Rev. B 26 (1982) p.4199.

[22] L. Kleinman and D.M. Bylander, Phys. Rev. Lett. 48 (1982) p.1425.

[23] D. Vanderbilt, Phys. Rev. B 41 (1990) p.7892.

[24] N. Troullier and J.L. Martins, Phys. Rev. B 43 (1991) p.1993.

[25] S.G. Louie, S. Froyen, and M.L. Cohen, Phys. Rev. B 26 (1982) p.1738.

[26] X. Gonze, R. Stumpf and M. Scheffler, Phys. Rev. B 44 (1991) p.8503.

[27] A. Philipetti, A. Satta, D. Vanderbilt and W. Zhong, Int. J. Quantum Chem. 61 (1997) p. 421

[28] S.R. Shenoy and N.C. Halder, Phys. Rev. B 11 (1975) p.690.

[29] F.S. Ham, Solid State Phys. 1 (1955) p.127.

[30] C.E. Moore, *Atomic Energy Levels*, National Bureau of Standards, Washington, D.C., (1949).

[31] A.O.E. Animalu and V. Heine, Phil. Mag. 12 (1965) p.1249.

[32] E.R. Cowley, Can. J. Phys. 54 (1976) p.2348.

[33] P. Nozières and D. Pines, Phys. Rev. 111 (1958) p.442.

[34] L.E. Ballentine and O.P. Gupta, Can. J. Phys. 49 (1971) p.1549.

[35] O. Ese and J.A. Reissland, J. Phys. F3 (1973) p.2066.

[36] M. Taut and G. Paasch, Phys. Stat. Sol. (b) 51 (1971) p. 295.

[37] J.J. Hallers, T. Marien and W. Van der Lugt, Physica. 78 (1974) p.259.

[38] C. Kittel, *Introduction to solid state physics*, 2nd ed., New York: Wiley, (1956), p.99.

[39] S. Hellal, *Thèse de Doctorat d'Etat*, Université de Tizi-Ouzou (Algérie), (2006).

[40] M. Appapillai and A.R. Williams, J. Phys. F 3 (1973) p.759.

[41] R.W. Shaw Jr, J. Phys. C2 (1969) p.2335.

[42] V. Hugouvieux, E. Farhi, M.R. Johnson, F. Juranyi, P. Bourges and W. Kob, Phys. Rev. B 75, (2007) p.104208.

[43] M.J. Huijben and W. Van der Lugt, Acta Crys. A 35 (1979) p.431.

[44] A.J. Greenfield, J. Wellendorf and N. Wiser, Phys. Rev. A 4 (1971) p.1607.

[45] H. Olbrich, H. Ruppersberg and S. Steeb, Z. Narturf. A 38 (1983) p.1328.

[46] K.N. Lad and A. Pratap, Phys. Rev. B 73 (2006) p.054204.

[47] U. Balucani and M. Zoppi, *Dynamics of the Liquid State* (Clarendon Press, Oxford, 1994).

[48] R.E. Meyer and N.H. Nachtrieb, J. Chem. Phys. 23 (1955) p.1851.

[49] J. Röhlin and A. Lodding, Z. Naturforsch. 17a (1962) p.1081.

[50] C.C. Hsu and H. Eyring, Proc. Nat. Acad. Sci. 69 (1972) p.1342.

Figure captions

fig. 1. Influence of the OMP-model parameters $A_\ell(E)$ upon the interatomic potential behaviour for liquid sodium. Our calculations are performed at T=378K according to the following schemes: OMP-Self (continuous line), OMP-AH (dashed line), OMP-BG1 (dotted line), or OMP-BG2 (dash-dot-dotted line).

fig. 2. Influence of the OMP-model parameters $A_\ell(E)$ upon the pair-correlation function $g(r)$ for liquid sodium issued from molecular dynamics simulation with the corresponding interatomic potentials of fig. 1. Theoretical $g(r)$ curves with caption as for Fig. 1, are compared to the experiment of Waseda [6] (open circle).

fig. 3. Influence of the OMP-model parameters $A_\ell(E)$ upon the structure factor $S(q)$ for liquid sodium calculated from the corresponding $g(r)$ of fig. 2 (with same caption). The experimental values are those of Huijben and Van der Lugt [43] (open circles) and those of Greenfield *et al.* [44] (open squares)

fig. 4. Interatomic pair potentials for the liquid alkali metals near the melting point evaluated with OMP-Self: Li (dashed line), Na (continuous line) and K (dotted line).

fig. 5. Structure factor S(q) of liquid lithium at 463K calculated from OMP-model potential with OMP-Self, is first obtained by Fourier transform of pair correlation function with 4000 particles (continuous line) and also from direct MD-calculation with 864 particles (solid squares) by using (equation 3. 3 in the text). Experimental values are those of Waseda [6] (open circles) and those of Olbrich *et al.* [45] (open triangles).

fig. 6. Structure factor S(q) of liquid potassium at 338K calculated from OMP-model potential with OMP-Self, is first obtained by Fourier transform of pair correlation function with 4000 particles (continuous line) and also from direct MD-calculation with 864 particles (solid squares) by using (equation 3. 3 in the text). Experimental values are those of Greenfield *et al.* [44] (open triangles) and those of Waseda [6] (open circles).

fig. 7. Normalized VAF for Li, Na, and K as a function of temperature calculated with the full-nonlocally screened OMP-model potential with self-consistent core shift (OMP-Self).

fig. 8. Spectral density of VAF for Li, Na, and K, normalized to a unit area. Same legend as fig. 7.

fig. 9. Self-diffusion coefficients as a function of temperature calculated with the full-nonlocally screened OMP-model potential with self-consistent core shift (OMP-Self). The open and solid triangles correspond the experiments values for Na [48] and for K [49], respectively. (a) represent previous calculations with other potentials for Li [50], Na [50], and K [50]. (b) correspond to our calculations. Note that Ln(D) is plotted versus 10^{-3} / T

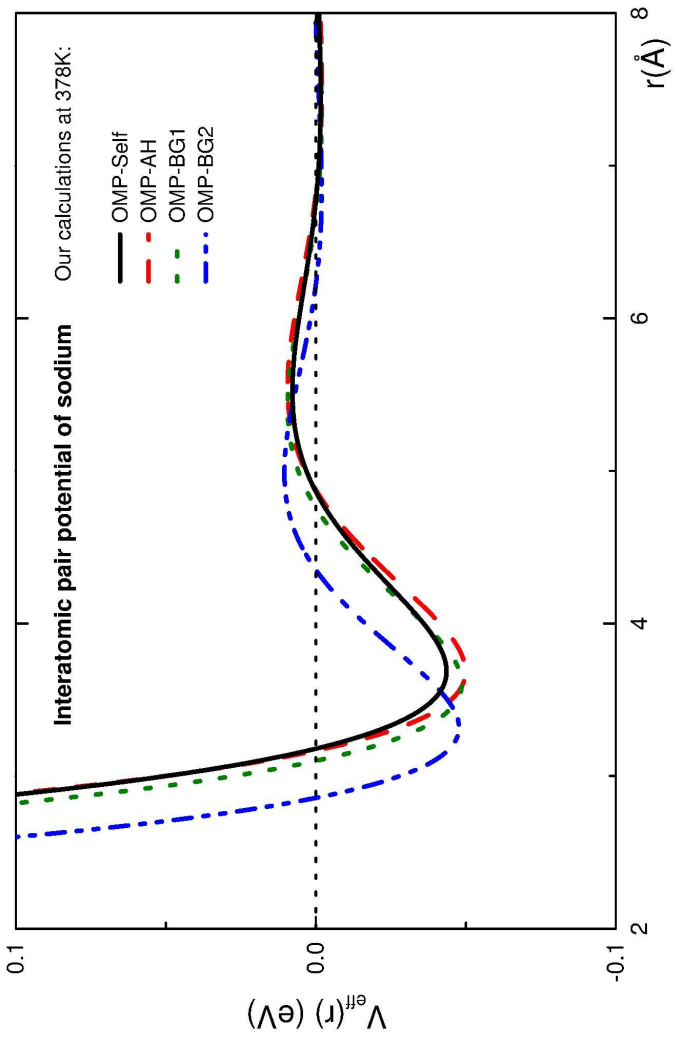

209x297mm (600 x 600 DPI)

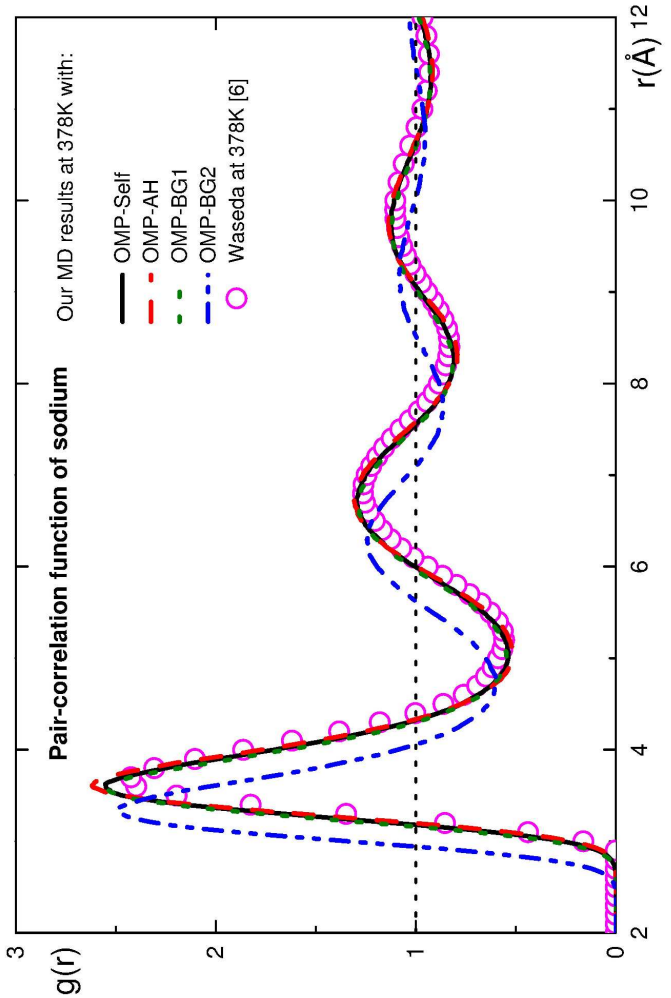

209x297mm (600 x 600 DPI)

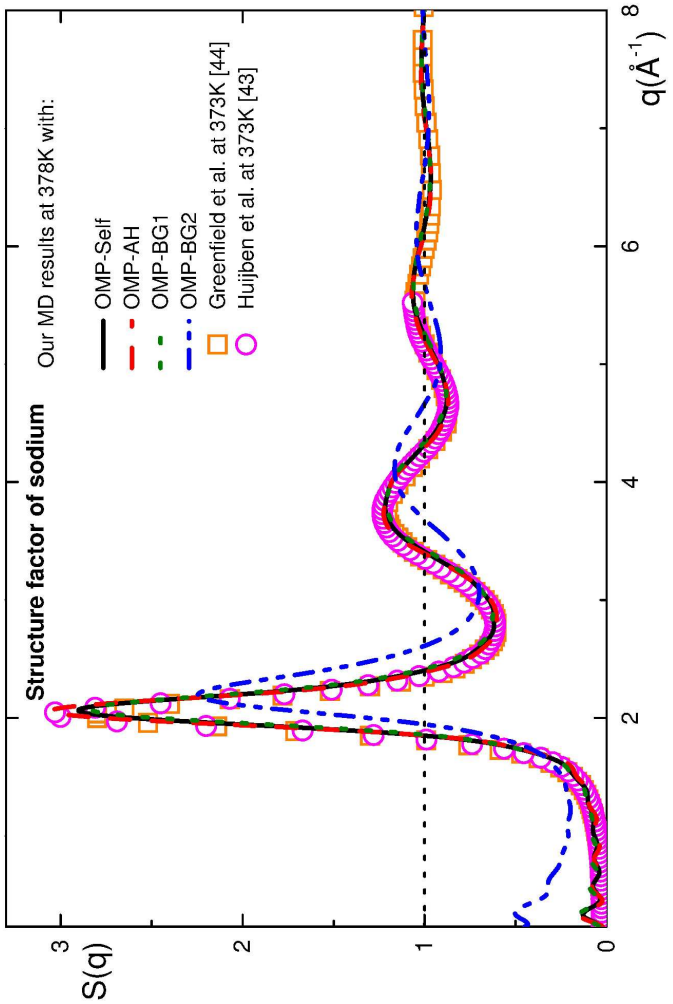

209x297mm (600 x 600 DPI)

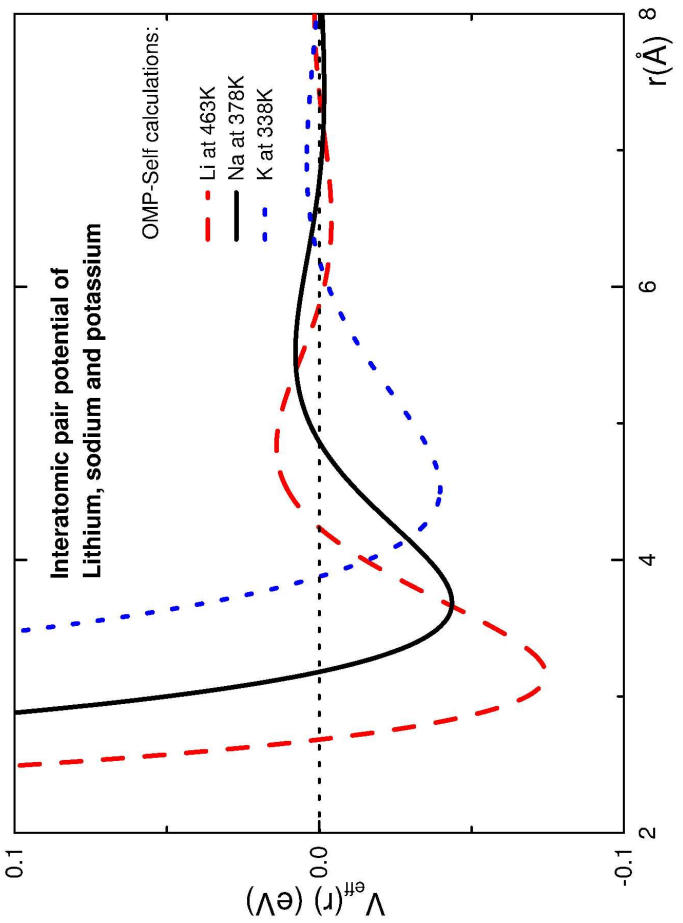

209x297mm (600 x 600 DPI)

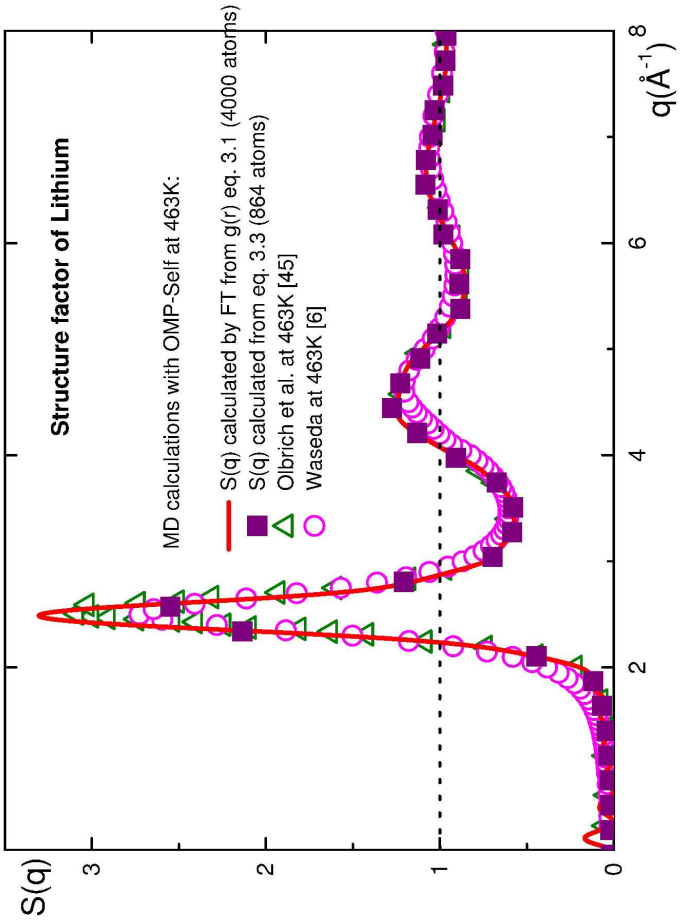

209x297mm (600 x 600 DPI)

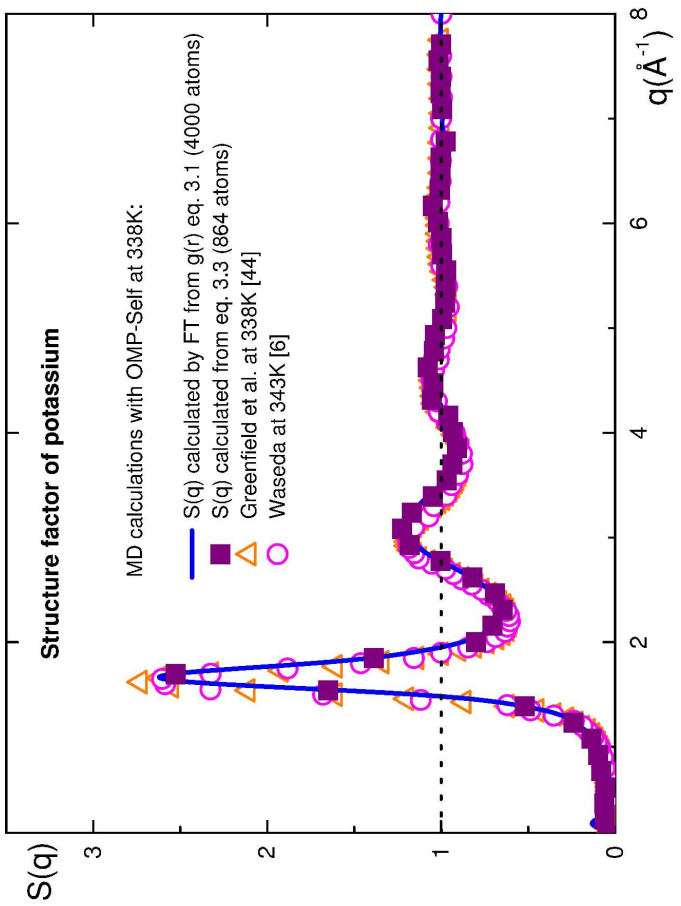

209x297mm (600 x 600 DPI)

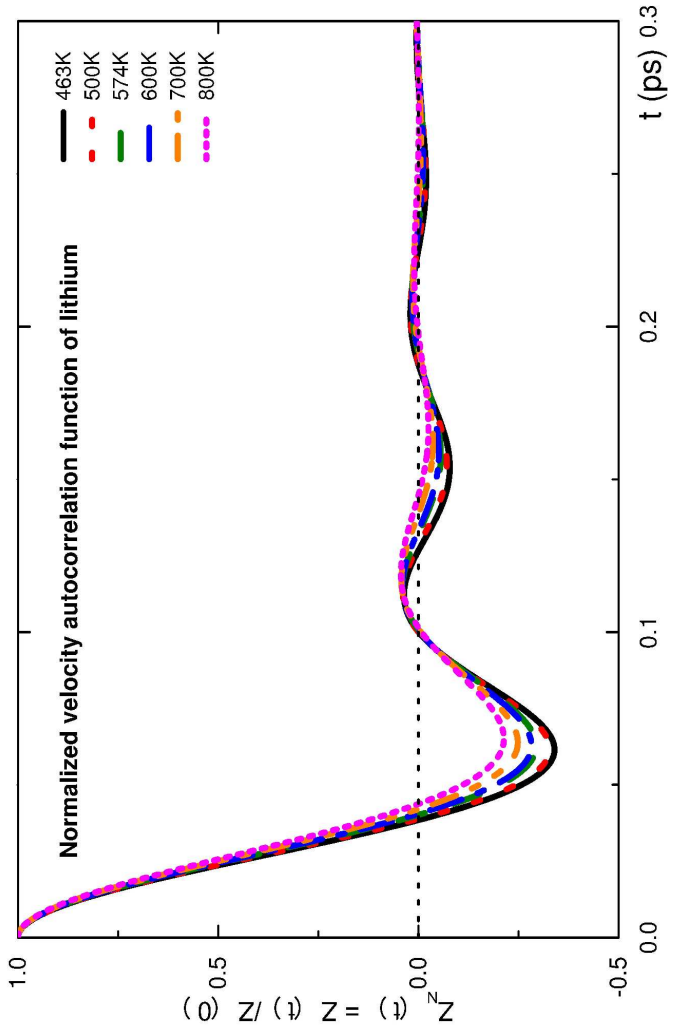

209x297mm (600 x 600 DPI)

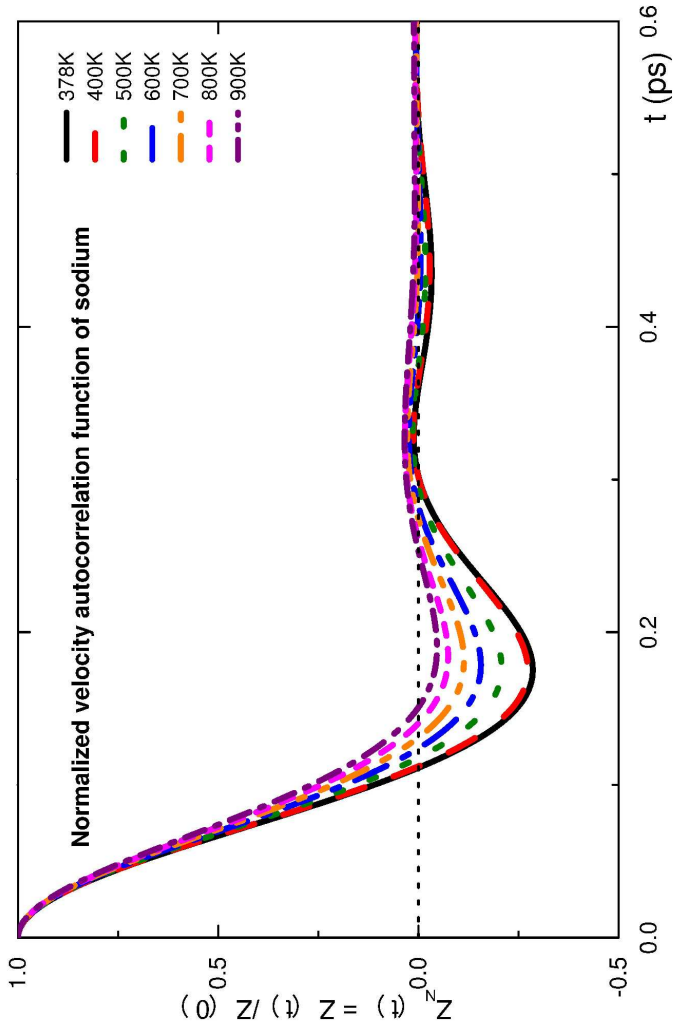

209x297mm (600 x 600 DPI)

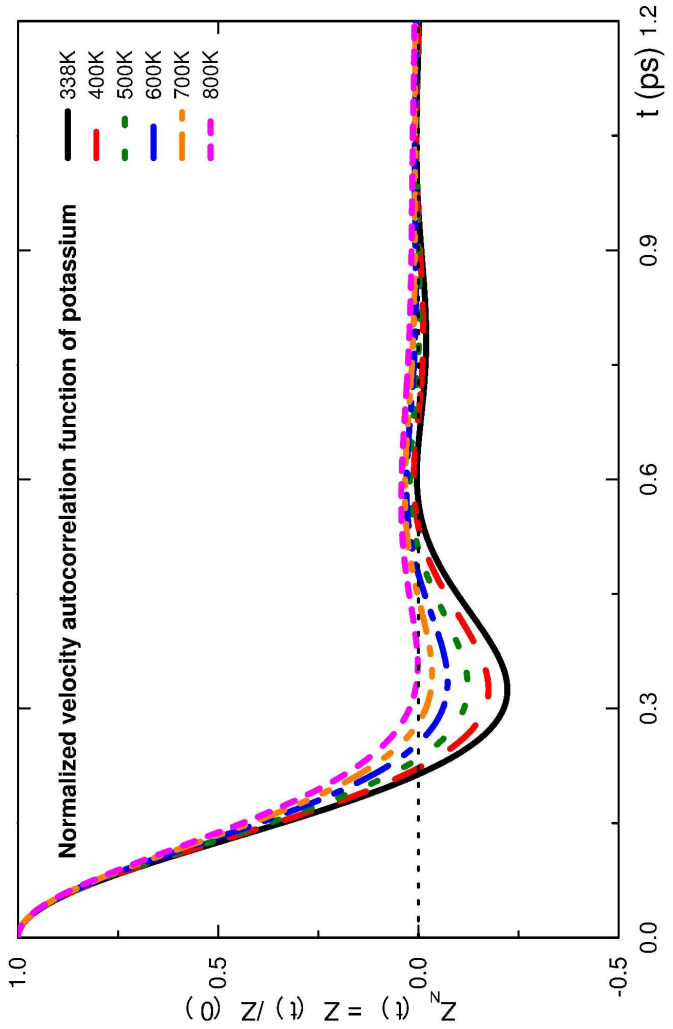

209x297mm (600 x 600 DPI)

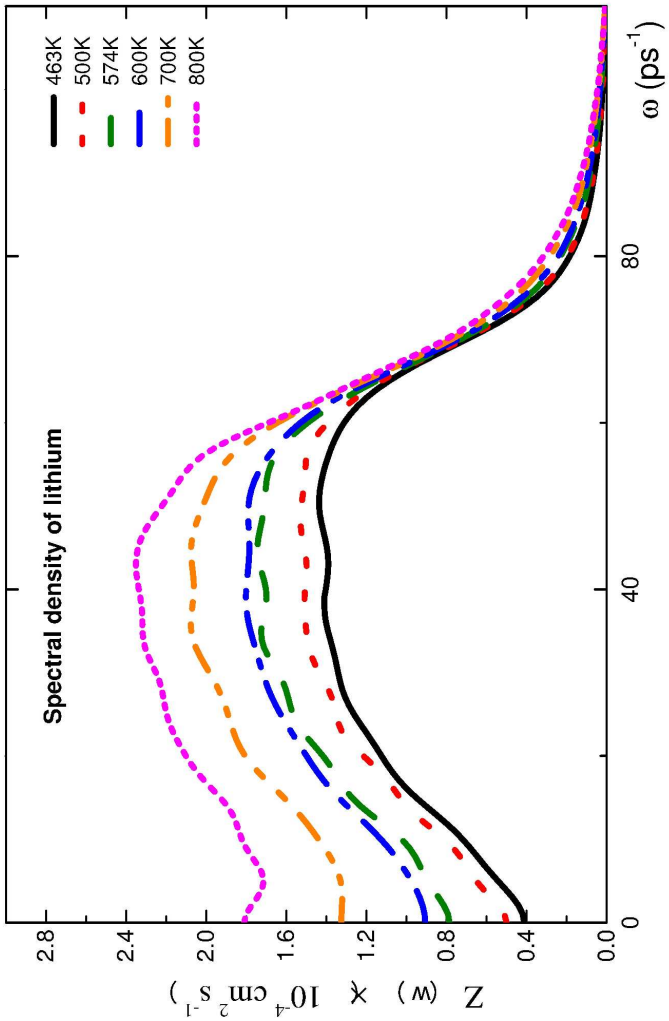

209x297mm (600 x 600 DPI)

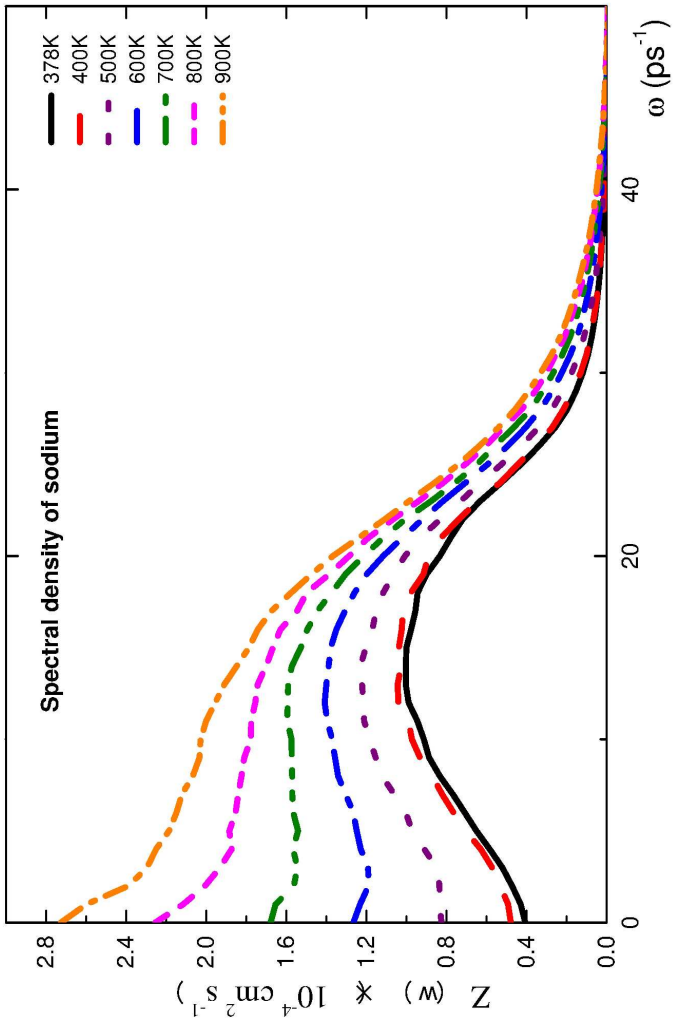

209x297mm (600 x 600 DPI)

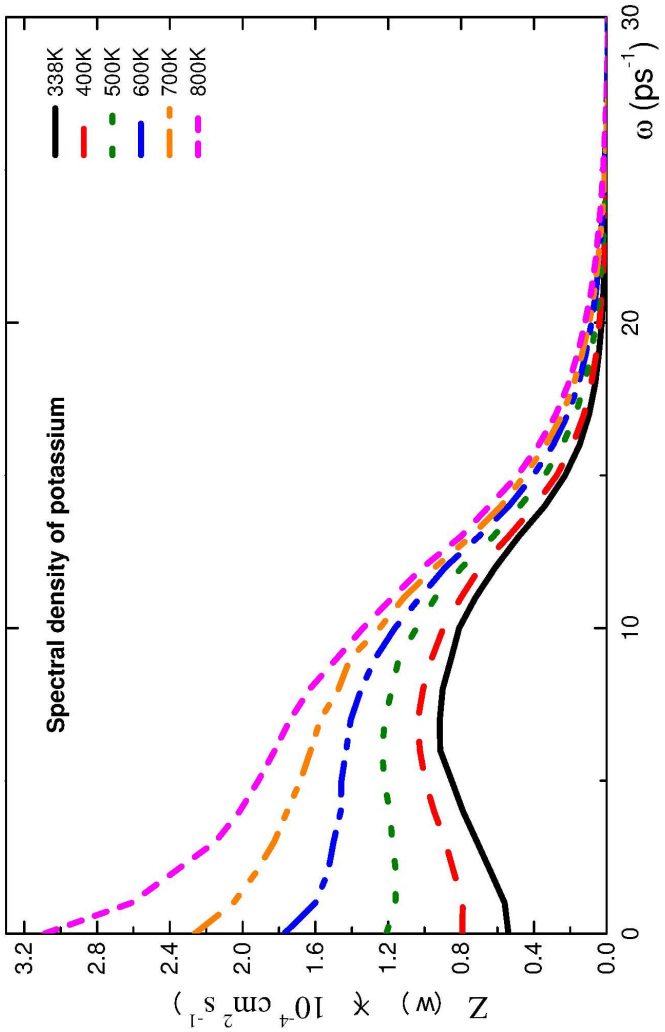

209x297mm (600 x 600 DPI)

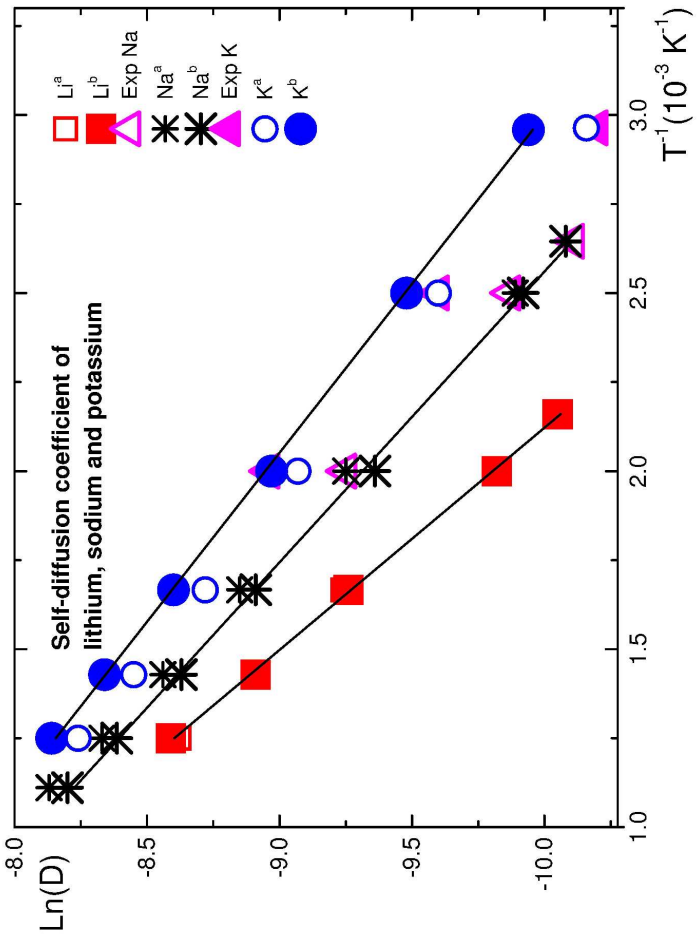

209x297mm (600 x 600 DPI)

Table I. OMP parameters determined at the shifted Fermi energy level E_F^* according to our self-consistent calculation of the core shift (OMP-Self: first line) along with previous calculations related to other procedures devised by Cowley [Ref. 32]. The second line corresponds to the use of Animalu-Heine's method (OMP-AH) [Ref. 31]. The third and fourth lines refer to like this method but with respectively the first correction (OMP-BG1) and the second one including "inhomogeneity correction" (OMP-BG2) that were both suggested by Ballentine and Gupta [Ref. 34]. On the other hand, the last column shows the calculated bonding energy BEE (a) that is compared to available experimental data taken from [Ref. 35] (b) or from [Ref. 38] (c). All values are in atomic units.

	T (K)	r_s	$A_0\left(E_F^*\right)$	$\frac{\partial A_0}{\partial E}$	$A_1\left(E_F^*\right)$	$\frac{\partial A_1}{\partial E}$	BEE
Li	463	3.306	0.326 (OMP-Self)	-0.1829			0.0612 [a]
			0.326 (OMP-AH)	-0.1829			0.0582 [b]
			0.341 (OMP-BG1)	-0.1829			0.0606 [c]
			0.381 (OMP-BG2)	-0.1829			
Na	378	4.016	0.305 (OMP-Self)	-0.2291	0.361 (OMP-Self)	-0.0970	0.0366 [a]
			0.307 (OMP-AH)	-0.2291	0.362 (OMP-AH)	-0.0970	0.0414 [b]
			0.318 (OMP-BG1)	-0.2291	0.367 (OMP-BG1)	-0.0970	0.0415 [c]
			0.364 (OMP-BG2)	-0.2291	0.386 (OMP-BG2)	-0.0970	
K	338	5.016	0.247 (OMP-Self)	-0.3118	0.259 (OMP-Self)	-0.1657	0.0467 [a]
			0.240 (OMP-AH)	-0.3118	0.255 (OMP-AH)	-0.1657	0.0360 [b]
			0.254 (OMP-BG1)	-0.3118	0.263 (OMP-BG1)	-0.1657	0.0346 [c]
			0.306 (OMP-BG2)	-0.3118	0.290 (OMP-BG2)	-0.1657	

[a] Our calculations
[b] Taken from Ref. [35]
[c] Taken from Ref. [38]

Table II.

	T(K)	D ($\times 10^{-4}$ cm^2 s^{-1})	D_0 ($\times 10^{-4}$ cm^2 s^{-1})	Q (KJ /mol)
Li	463	0.507	13.603	13.323
		0.61-0.68[a]		12.442[b]
Na	378	0.436	10.442	10.182
		0.406-0.435[a]		10.137[b]
K	343	0.398	10.719	8.762
		0.359-0.376[a]		9.218[b]

[a] Taken from Ref. [47]
[b] Taken from Ref. [4]